

ARTICLE



Changes in the structural brain connectome over the course of a nonrandomized clinical trial for acute mania

Du Lei^{1,5}✉, Wenbin Li^{1,2,3,5}, Maxwell J. Tallman¹ , Stephen M. Strakowski⁴, Melissa P. DelBello¹, L. Rodrigo Patino¹, David E. Fleck¹, Su Lui¹ , Qiyong Gong¹ , John A. Sweeney^{1,2} , Jeffrey R. Strawn¹, Fabiano G. Nery¹, Jeffrey A. Welge¹, Emily Rummelhoff¹ and Caleb M. Adler¹

© The Author(s), under exclusive licence to American College of Neuropsychopharmacology 2022

Disrupted topological organization of brain functional networks has been widely reported in bipolar disorder. However, the potential clinical implications of structural connectome abnormalities have not been systematically investigated. The present study included 109 unmedicated subjects with acute mania who were assigned to 8 weeks of treatment with quetiapine or lithium and 60 healthy controls. High resolution 3D-T1 weighted magnetic resonance images (MRI) were collected from both groups at baseline, week 1 and week 8. Brain networks were constructed based on the similarity of morphological features across brain regions and analyzed using graph theory approaches. At baseline, individuals with bipolar disorder illness showed significantly lower clustering coefficient (C_p) ($p = 0.012$) and normalized characteristic path length (λ) ($p = 0.004$) compared to healthy individuals, as well as differences in nodal centralities across multiple brain regions. No baseline or post-treatment differences were identified between drug treatment conditions, so change after treatment were considered in the combined treatment groups. Relative to healthy individuals, differences in C_p , λ and cingulate gyrus nodal centrality were significantly reduced with treatment; changes in these parameters correlated with changes in Young Mania Rating Scale scores. Baseline structural connectome matrices significantly differentiated responder and non-responder groups at 8 weeks with 74% accuracy. Global and nodal network alterations evident at baseline were normalized with treatment and these changes associated with symptomatic improvement. Further, baseline structural connectome matrices predicted treatment response. These findings suggest that structural connectome abnormalities are clinically significant and may be useful for predicting clinical outcome of treatment and tracking drug effects on brain anatomy in bipolar disorder.

Clinical Trials Registration: Name: Functional and Neurochemical Brain Changes in First-episode Bipolar Mania Following Successful Treatment with Lithium or Quetiapine. URL: <https://clinicaltrials.gov/>. Registration number: NCT00609193. Name: Neurofunctional and Neurochemical Markers of Treatment Response in Bipolar Disorder. URL: <https://clinicaltrials.gov/>. Registration number: NCT00608075.

Neuropsychopharmacology (2022) 47:1961–1968; <https://doi.org/10.1038/s41386-022-01328-y>

INTRODUCTION

Despite the significant morbidity, and mortality associated with bipolar disorder, its pathophysiology remains poorly understood. Moreover, while the available pharmacotherapeutics for bipolar mania have demonstrated efficacy, their mechanisms of action remain to be fully understood. Obtaining neuroimaging data prior to, and during the course of treatment provides an opportunity to more directly evaluate the effects of treatment on brain networks, and potentially to identify pretreatment brain features that predict treatment response [1, 2].

Developments in systems neuroscience have documented that the human brain is comprised of interconnected networks with distinct behavioral relevance. Psychiatric symptoms, such as manic

episodes in bipolar illness may represent a disruption of normal integration amongst these cortical and subcortical brain regions [3–7], and these alterations may predict and normalize in relation to treatment outcome [8–10].

Graph-based theoretical analysis provides a powerful framework for characterizing topological properties of brain networks [11–14]. In this approach, the brain is modeled as a network composed of a number of nodes and edges connecting the nodes. Nodes represent individual cortical and subcortical regions, and the edges reflect their connectivity, which is needed for information transfer within and between networks. High-resolution structural MRI has been increasingly used to delineate whole-brain connectivity patterns by evaluating patterns of

¹Department of Psychiatry and Behavioral Neuroscience, University of Cincinnati College of Medicine, Cincinnati 45219 OH, USA. ²Huaxi MR Research Center (HMRR), Department of Radiology, The Center for Medical Imaging, West China Hospital of Sichuan University, Chengdu 610041 Sichuan, P.R. China. ³Department of the Magnetic Resonance Imaging, The First Affiliated Hospital of Zhengzhou University, Zhengzhou 450052 Henan, P.R. China. ⁴Department of Psychiatry & Behavioral Sciences, Dell Medical School of The University of Texas at Austin, Austin 78712 TX, USA. ⁵These authors contributed equally: Du Lei, Wenbin Li. ✉email: alien18@163.com

Received: 14 December 2021 Revised: 17 March 2022 Accepted: 11 April 2022
Published online: 18 May 2022

interregional gray matter (GM) volume measurements [15–18]. Such measures can help to understand how alterations in network anatomy are related to the neurofunctional and behavioral characteristics associated with bipolar disorder [19, 20], and have been used to detect topological differences in brain networks of individuals across different psychiatric disorders [18, 21, 22]. Moreover, there have been recent report that alteration of connectome structure has value in identifying and predicting treatment response in psychotic disorders [23].

In this study, we employed graph-based analysis to examine anatomic brain networks of acutely manic individuals at baseline, and over 1 and 8 weeks of treatment with either quetiapine or lithium. Analyses utilized a recently developed approach in which interregional similarities of regional brain gray matter volume measurements are used to identify structural brain networks [24, 25]. Based on previous studies in bipolar disorder by Xia and colleagues who found greater randomization in network configuration, represented by lower clustering coefficient (C_p) and characteristic path length (λ) [26], we hypothesized that: (i) untreated individuals with bipolar mania would demonstrate less coherent network configuration than healthy subjects, represented by differences in neuroanatomic network measures; (ii) these topological differences would be reduced with treatment, with changes positively correlating with treatment response; and (iii) structural connectome findings would differ between those individuals with bipolar disorder who responded to 8 weeks of treatment and those who did not respond.

METHODS

Participants

This study was approved by the University of Cincinnati Institutional Review Board. All participants were evaluated clinically and using the Structured Clinical Interview for DSM-IV, Patient version (SCID-P) or the Washington University in St. Louis Kiddie Schedule for Affective Disorders and Schizophrenia (KSADS) [27]; manic symptoms were assessed with the Young Mania Rating Scale (YMRS) [28]. We enrolled 121 individuals (age range 16–55) meeting DSM-IV criteria for bipolar I disorder, from inpatient and outpatient services or by referral from community psychiatrists; all had an index YMRS total score ≥ 20 . Of the 121 patients enrolled, data from seven in the lithium treatment group and five in quetiapine treatment group were lost to follow-up due to reasons including: moving out of town, lack of efficacy, withdrawal of consent, medication noncompliance, and adverse events. Statistical analysis of treatment effects only included the 109 patients who complete the clinical trial and provided usable MRI scan data at all time points.

We also recruited 60 healthy individuals from the communities where patients resided. All included healthy individuals had three MRI and clinical evaluations paralleling those of the patients, and had no known history of mood or psychotic disorders personally or in their first- or second-degree relatives. All participants were physically healthy based on a medical interview and a physical exam and were excluded for any substance use disorder with the exception of nicotine. Additional clinical information including lifetime comorbidity, lifetime medication exposure, smoking status, and body mass index are presented in Supplementary Materials (Supplementary Table S1). Written informed consent was obtained from all participants, or their legal guardian prior to their participation; written assent was obtained from all participants under age 18 years of age.

Treatment procedures

Following clinical evaluation and MRI scanning, subjects with bipolar disorder received treatment with quetiapine ($n = 43$) or lithium ($n = 66$), and followed clinically over 8 weeks as previously described. Lithium target dose was based on achieving serum levels of 0.8–1.2 mEq/L; the maximum level allowed was 1.5 mEq/L. Quetiapine was flexibly dosed with a target daily dose of 100 mg on day 1, 200 mg by day 2, 300 mg by day 3, and 400 mg by day 4. Quetiapine could be titrated to 600 mg on day 5, and to a maximum of 800 mg on subsequent days, or decreased to a minimum of 200 mg, at the clinician's discretion. Treatment outcome was assessed using scores from the YMRS; response was defined as a $\geq 50\%$ reduction in YMRS scores from baseline.

Data acquisition

MRI acquisitions were performed on a 4 Tesla (4T) Varian Unity INOVA scanner with a 12-channel head coil as previously described [10, 29]. Earplugs and headphones were provided to block background noise, and foam padding around the head minimized head motion. Participants were scanned at three time points, at baseline (prior to treatment for patients), week 1, and week 8.

Following a three-plane gradient echo scan for alignment and localization, a shim procedure was performed to generate a homogeneous magnetic field. High resolution T1-weighted three-dimensional images were acquired with a Modified Driven Equilibrium Fourier Transform (MDEFT) protocol, optimized for the 4 T Varian scanner [Tau (magnetization preparation time) = 1.1 s, TR = 13 ms, TE = 5.3 ms, field of view = 192 mm \times 256 mm \times 256 mm, matrix = 192 \times 256 \times 256, flip angle = 20 degrees, slice thickness = 1 mm] as previously described [10, 29–31]. T1-weighted images were visually inspected to identify scans with excessive motion artifact for exclusion. No scanning artifacts or gross brain abnormalities were observed in any participant included in analyses.

MRI data preprocessing

Structural images were processed using Statistical Parametric Mapping software (SPM 12; <http://www.fil.ion.ucl.ac.uk/spm>). In brief, individual structural images were first segmented into gray matter (GM), white matter (WM), and cerebral spinal fluid (CSF) using the unified segmentation model [32]. The resulting GM maps were then normalized to Montreal Neurological Institute (MNI) space using a high-dimensional “DARTEL” approach and subjected to nonlinear modulation to compensate for spatial normalization effects. Finally, the GM data were re-sampled to 1.5 mm³ voxels and spatially smoothed (Gaussian kernel with a full width at half maximum of 6 mm).

Construction of structural networks and calculation of network properties

We used the automated anatomical labeling (AAL) algorithm to parcellate GM into 90 non-cerebellar anatomical regions-of-interest (ROIs) representing network “nodes” [33]. Edges represent the morphological connections between nodes. The well-established Kullback-Leibler divergence-based similarity (KLS) index was utilized to characterize the connections or edges between anatomic regions [10, 24]. In short, higher similarity in gray matter density distribution between two anatomical regions is represented by higher KLS scores; suggesting stronger connections and shorter edges between regions. The range of KLS is from 0 to 1, with 1 representing an identical density distribution for two regions. We calculated the KLS values between all possible pairs of 90 brain regions, generating a 90 \times 90 similarity matrix for each subject. In this 90 \times 90 network matrix, each row and column represent a brain region and each element represents the similarity of morphological distributions between a pair of brain regions.

Thresholding of correlation matrices reveal different topological properties and which may obscure putative group differences [34]. Determining a threshold involves a tradeoff between a sparse network (low threshold) and a highly linked one (high threshold). To avoid the bias coming from choosing single threshold level, we applied a wide range of sparsity (S) thresholds to all correlation matrices. The parameter S was determined ensuring that thresholded networks were estimable for the small-worldness scalar and that the small-world index (σ) was larger than 1.0 [35]. The range of S parameters thus determined was 0.10 $< S <$ 0.34 with an interval of 0.01. For each network metric, the area under the curve (AUC), which provides a summarized scalar for the topological characterization of brain networks independent of a single threshold selection, was calculated. The AUC metric has been proven to be sensitive in detection of topological alterations of brain networks [36, 37].

Based on those thresholded weighted matrices, both global and nodal network properties were calculated for brain networks. The global metrics, including small-world parameters and network efficiency [38, 39], were examined as follows: small-world parameters included clustering coefficient (C_p), characteristic path length (L_p), normalized clustering coefficient (γ), normalized characteristic path length (λ), and small worldness (σ). The network efficiency parameters included local efficiency (E_{loc}) and global efficiency (E_{glob}). Node metrics obtained included nodal degree [34], nodal efficiency [38], and betweenness centrality [40]. More details of structural network construction and topological metrics calculation are included in Supplementary Materials.

As we had multiple scans on HC, we computed the intraclass correlation coefficient (ICC) of topological measurements to assess consistency of

Table 1. Demographics and clinical characteristics of the participants.

	Bipolar disorder (N = 109)	Healthy controls (N = 60)	
Age (years \pm SD(range))	25 \pm 10 (17–52)	23 \pm 5 (17–53)	$p = 0.098^a$
Male (%)	46 (42%)	29 (48%)	$p = 0.443^b$
	Lithium (N = 66)	Quetiapine (N = 43)	
Age (years \pm SD)	26 \pm 11	24 \pm 8	$p = 0.20^a$
Male (%)	24 (36%)	22 (51%)	$p = 0.13^b$
YMRS (Baseline \pm SD)	23.5 \pm 6.9	24.5 \pm 6.2	$p = 0.50^a$
YMRS (week 1 \pm SD)	13.8 \pm 6.7	15.2 \pm 7.2	$p = 0.33^a$
YMRS (end point \pm SD)	10.1 \pm 6.6	10.3 \pm 7.6	$p = 0.83^a$
Responders at week 1 N (%)	27 (40.9%)	14 (32.6%)	$p = 0.38^b$
Responders at end point N (%)	42 (63.6%)	25 (58.1%)	$p = 0.332^b$

YMRS Young mania rating scale

^aIndependent-sample t test.

^bChi-squared test.

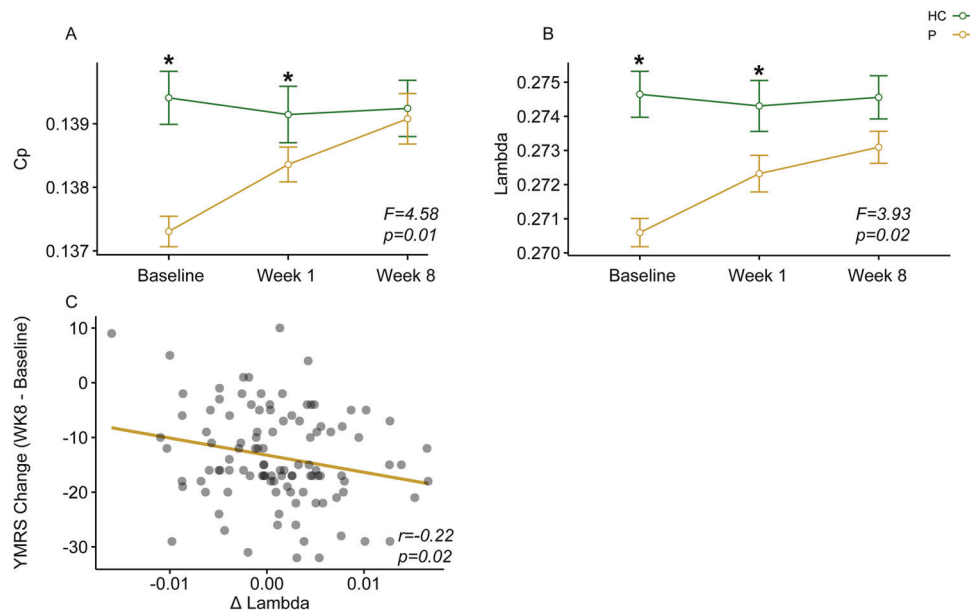


Fig. 1 Change in global network measures over the course of treatment and correlation to YMRS change in individuals with bipolar disorder. **A** Clustering coefficient showed significant group-by-time interaction effects ($F = 4.58$, $p = 0.01$). **B** Normalized characteristic path length (λ) showed significant group-by-time interaction effects ($F = 3.93$, $p = 0.02$). **C** Normalized characteristic path length (λ) significantly correlated with changes in YMRS score ($r = -0.22$, $p = 0.02$). *Clustering coefficient (C_p) and normalized characteristic path length (λ) significantly differed between bipolar and healthy subjects at baseline (C_p : $p = 0.01$, λ : $p < 0.01$) and week 1 (C_p : $p = 0.01$, λ : $p = 0.03$). There were no significant differences in global brain network properties between groups at week 8. Quantitative data were demonstrated as mean \pm standard error. HC Healthy individuals, P Patients with bipolar disorder, WK Week, YMRS Young Mania Rating Scale.

these measures over time in the healthy control group. Results of this analysis are presented in Supplementary Table S2.

Statistical analysis

Using MATLAB (www.mathworks.com), we applied nonparametric permutation tests to identify significant between-group differences in the AUC of network metrics [37]. Baseline values in global and nodal network properties of structural connectomes were compared between bipolar and healthy individuals. We randomly reallocated all values for each network metric into two groups and recomputed the mean differences between them. This randomization procedure was repeated 10,000 times, and the 95th percentile of each distribution was used as the critical value for a two-tailed test of the null hypothesis with a type I error of 0.05. The Benjamini-Hochberg false discovery rate (FDR) correction was applied to testing for differences in nodal measures.

To determine whether medication treatment had significant effects on topological measurements (all bipolar group vs control group), group-by-time interaction effects were tested using mixed effects models.

To test for changes in patients over the course of treatment, the primary analysis tested for significant normalization of alterations present at baseline, considering data from all three time points simultaneously. Correlations between changes in network measurements and changes in manic symptoms (YMRS) were examined, treating both age and sex as covariates. Similar analyses controlling for baseline YMRS scores were also conducted in the bipolar patients. In order to test for differences between quetiapine and lithium treatment on topological alterations, drug-by-time interaction effects within the bipolar group were examined using mixed effects models for global and nodal measurements that were altered relative to controls at baseline. In supplemental analyses, as smoking status and body mass index may impact changes of topological measurements, we tested the effects of these two variables on treatment-related changes using a general linear model.

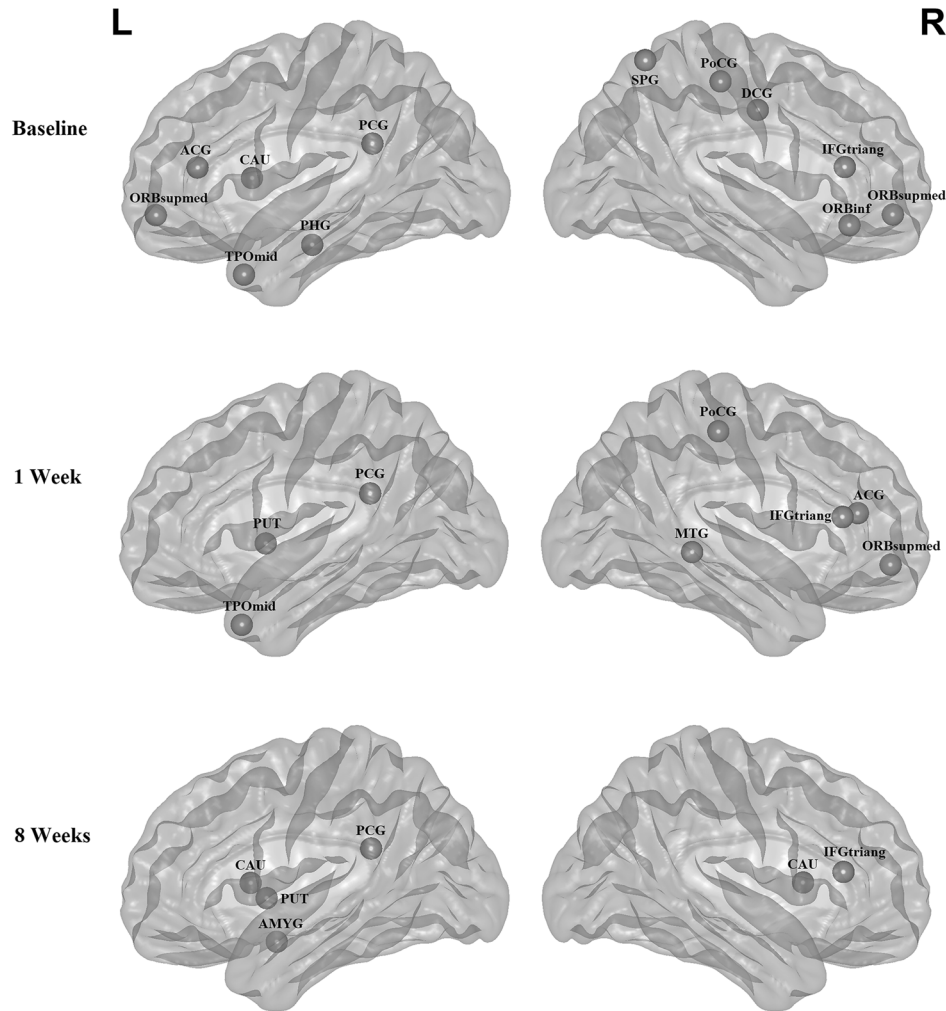


Fig. 2 Nodal centrality differences between bipolar and healthy subjects across time points. The nodes were mapped onto the cortical surfaces by using the BrainNet Viewer package (<http://www.nitrc.org/projects/bnv>). The nodal centrality differences between bipolar and healthy subjects at baseline did not survive application of an FDR threshold of $q = 0.05$, so the nodal results are presented with nominal significance thresholds for heuristic purposes. IFGtriang Inferior frontal gyrus, triangular part, ORBinf Inferior frontal gyrus, orbital part, ORBsupmed Superior frontal gyrus, medial orbital, ACG Anterior cingulate and paracingulate gyri, DCG Median cingulate and paracingulate gyri, PCG Posterior cingulate gyrus, PHG Parahippocampal gyrus, PoCG Postcentral gyrus, SPG Superior parietal gyrus, CAU Caudate, TPOmid Temporal pole: middle temporal gyrus, PUT Putamen, MTG Middle temporal gyrus, AMYG Amygdala. R = right hemisphere; L = left hemisphere.

Finally, we compared baseline connectome measures of treatment responders and non-responders. As a strategy for examining whether baseline structural connectome measures considered together can predict treatment response at week 8, we applied support vector machine (SVM) to the preprocessed GM images, as well as the whole connectome-wide matrices (90×90 Pearson correlation matrix). Statistical significance was estimated using the permutation method (1000 permutations). The methods used for these analyses are described in detail in Supplementary Materials.

RESULTS

Demographic and clinical characteristics

Bipolar and healthy subjects did not significantly differ in either sex or age, nor did they differ between bipolar subjects receiving quetiapine or lithium treatment. Quetiapine and lithium groups did not differ in YMRS score at baseline, week 1, or week 8 (Table 1).

There were no significant treatment-by-time interaction effects for YMRS scores between lithium and quetiapine ($F = 0.14$, $p = 0.87$). In addition, medication response, defined as a 50% decrease

in YMRS score, did not differ between participants treated with quetiapine or lithium (Table 1).

Alterations of brain network properties at baseline

In the defined threshold range, both bipolar and healthy subjects showed small-world topology in brain structural connectomes at baseline. However, the bipolar group showed significantly lower C_p ($p = 0.012$) and λ ($p = 0.004$) at baseline (Fig. 1A, B) than controls, but the groups did not significantly differ in L_p ($p = 0.27$), γ ($p = 0.69$), σ ($p = 0.71$), E_{loc} ($p = 0.074$), or E_{glob} ($p = 0.43$).

Nodal centrality differences between bipolar and healthy subjects at baseline did not survive application of an FDR threshold of $q = 0.05$, but nodal results are noted with nominal significance thresholds for heuristic purposes. Brain regions that showed these nominal between-group differences in nodal parameters at baseline included bilateral superior frontal gyrus (medial orbital aspect), right inferior frontal gyrus (triangular and orbital part), right middle cingulate and paracingulate gyri, right postcentral gyrus, right superior parietal gyrus, left anterior cingulate and paracingulate gyri, left posterior cingulate gyrus,

Table 2. Regions showing differences in nodal centralities between bipolar and health subjects across different time points.

Brain regions	Nodal degree	P Values	
		Nodal efficiency	Nodal betweenness
Baseline			
R Inferior frontal gyrus, triangular	0.934	0.820	<0.001 ↓
R Inferior frontal gyrus, orbital	0.027 ↑	0.029 ↑	0.007 ↑
L Superior frontal gyrus, medial orbital	0.055	0.251	0.044 ↑
R Superior frontal gyrus, medial orbital	0.050 ↑	0.043 ↑	0.092
L Anterior cingulate and paracingulate gyri	0.159	0.044 ↑	0.678
R Median cingulate and paracingulate gyri	0.451	0.320	0.042 ↑
L Posterior cingulate gyrus	0.224	0.044 ↓	0.583
L Parahippocampal gyrus	0.289	0.384	<0.001 ↓
R Postcentral gyrus	<0.001 ↓	<0.001 ↓	0.023 ↓
R Superior parietal gyrus	<0.001 ↓	<0.001 ↓	0.142
L Caudate	0.087	0.119	0.035 ↑
L Temporal pole: middle temporal gyrus	0.014 ↑	0.063	0.829
Week 1			
R Inferior frontal gyrus, triangular	0.133	0.104	0.016 ↓
R Superior frontal gyrus, medial orbital	0.331	0.046 ↑	0.047 ↑
R Anterior cingulate and paracingulate gyri	0.652	0.034 ↑	0.056
L Posterior cingulate gyrus	0.904	0.174	0.046 ↓
R Postcentral gyrus	0.562	<0.001 ↓	<0.001 ↓
L Putaman	0.529	0.003 ↑	<0.001 ↑
R Middle temporal gyrus	0.021 ↓	0.641	0.955
L Temporal pole: middle temporal gyrus	0.034 ↓	0.835	0.933
Week 8			
R Inferior frontal gyrus, triangular	0.295	0.412	0.010 ↓
L Posterior cingulate gyrus	0.691	0.685	0.012 ↓
L Amygdala	0.026 ↓	0.908	0.909
L Caudate	0.015 ↑	0.019 ↑	0.157
R Caudate	0.603	0.047 ↑	0.105
L Putaman	0.653	0.032 ↑	0.133

Regions were considered abnormal in the bipolar subjects if they exhibited significant between-group differences ($P < 0.05$, uncorrected) in any one of the three nodal centralities (shown in bold font). All brain regions are from automated anatomical labeling (AAL). ↑, bipolar subjects showed greater nodal centralities than control subjects; ↓, bipolar subjects showed lower nodal centralities than control subjects.

left parahippocampal gyrus, left caudate, and left temporal pole (Fig. 2 and Table 2).

Differences between quetiapine and lithium treatment

There were no significant differences in any network parameters between treatment groups at baseline (Supplementary Table S3), or significant treatment-by-time interaction effects in any global or nodal network parameters (Supplementary Table S4). Therefore, in further analyses of changes with treatment and symptomatic correlations the two drug treatment groups were combined.

Topological alterations after medication treatment

We observed significant changes in C_p ($F = 4.58$, $p = 0.01$) and λ ($F = 3.93$, $p = 0.02$) in bipolar subjects with treatment, with both measures normalizing toward HC over the course of the study (Fig. 1A, B). Subjects with bipolar disorder continued to show significantly lower C_p ($p = 0.01$) and λ ($p = 0.03$) versus healthy subjects at week 1 of treatment, but there were no significant differences between bipolar and healthy subjects in these or any other global brain network property at week 8. Individual trajectories of C_p and λ over time are provided in Supplementary Materials. Further, change in λ over 8 weeks of treatment was

significantly correlated with change in YMRS ratings ($r = -0.22$, $p = 0.02$) (Fig. 1C). Considering the baseline mania symptoms as an additional covariate did not meaningfully change this finding ($r = -0.19$, $p = 0.05$).

Bipolar participants showed progressively fewer brain regions with nominally significant differences from healthy subjects in nodal networks after 1 and 8 weeks of treatment (Fig. 2, Table 2). Nodal efficiency of left anterior cingulate ($F = 3.63$, $p = 0.03$) and left posterior cingulate gyri ($F = 4.12$, $p = 0.02$) showed nominally significant group-by-time interactions, in both case with bipolar participants demonstrating a relative normalization of nodal efficiency toward values of healthy participants (Fig. 3A, B). Moreover, changes in nodal efficiency of left anterior cingulate and left posterior cingulate gyri were significantly correlated with changes in YMRS scores (Fig. 3C, D). These relationships remained significant when considering baseline YMRS as a covariate (nodal efficiency of left anterior cingulate and paracingulate gyri [ACG]: $r = 0.26$, $p < 0.01$; nodal efficiency of left posterior cingulate gyrus [PCG]: $r = -0.27$, $p < 0.01$). Our general linear models also showed that changes of topological measurements were not significantly affected by body mass index or smoking status (Supplementary Tables S5, S6).

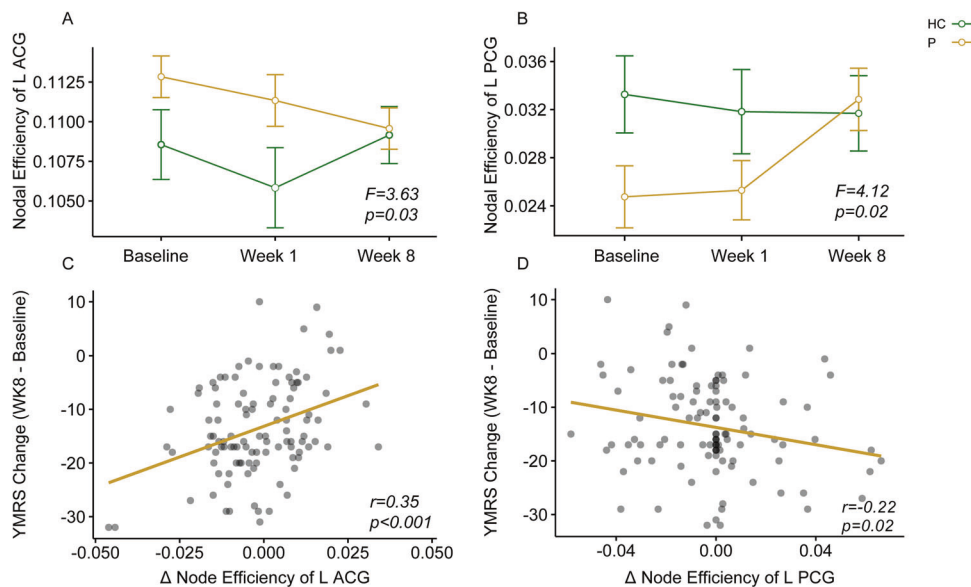


Fig. 3 Change in regional network measures over the course of treatment and correlation to YMRS change in individuals with bipolar disorder. **A** Nodal efficiency of left anterior cingulate showed significant group-by-time interaction effects ($F = 3.36$, $p = 0.03$). **B** Nodal efficiency of left posterior cingulate gyrus showed significant group-by-time interaction effects ($F = 4.12$, $p = 0.02$). **C** Changes in nodal efficiency of left anterior cingulate significantly correlated with changes in YMRS score ($r = 0.35$, $p < 0.001$). **D** Changes in nodal efficiency of left posterior cingulate significantly correlated with changes in YMRS score ($r = -0.22$, $p = 0.02$). ACG Anterior cingulate and paracingulate gyri, HC Healthy individuals, L Left, P Patients with bipolar disorder, PCG Posterior cingulate gyrus, WK Week, YMRS Young Mania Rating Scale.

Prediction of treatment outcome

We applied machine learning to baseline scan data to predict treatment outcome. Using baseline preprocessed smoothed gray matter images (voxel level), the balanced mean accuracy of classification of responders versus non-responders (58%) was only slightly higher than chance (sensitivity 75% and specificity 42%, $p = 0.04$). However, using connectome-wide matrices at baseline, we achieved a mean accuracy of 74% (sensitivity 57% and specificity 91%, $p < 0.05$).

DISCUSSION

We applied graph theory-based analysis methods to MRI structural images to identify and track changes in topological properties of GM networks, and the relationship of these changes to treatment outcome in acutely manic patients with bipolar disorder. Our findings indicate that at baseline, acute mania is associated with a more randomized structural brain network, reflected in lower clustering coefficient and lower normalized characteristic path length. Global network disruption also has been reported in other neuropsychiatric disorders including posttraumatic stress disorder [41], obsessive compulsive disorder [39], schizophrenia [42], and major depressive disorder [43], though with distinguishing specific characteristics. In addition, we observed a normalization of the identified neuroanatomic connectome alterations in clustering coefficient and normalized characteristic path length following acute treatment. Neuroanatomic normalization was correlated with reduction in mania symptom severity. These effects did not significantly differ between lithium and quetiapine therapy, suggesting that they represent downstream effects of the two drugs with different pharmacological mechanisms of action.

At the regional level, exploratory analyses of nodal alterations using nominal significance thresholds suggest altered nodal centralities in multiple brain regions. Although significance of these nodal-level findings does not survive correction for multiple comparisons, the large number of nominally significant differences between bipolar and healthy subjects is consistent with findings from our global network level analysis. Moreover, also consistent with our primary findings, the number of regions

showing between-group differences decreased with treatment. Of note, both left anterior and posterior cingulate gyri, regions implicated in cognitive and affective regulation, showed normalization of nodal efficiency with treatment that correlated with symptomatic improvement [44, 45].

While most changes after treatment involved narrowing of differences between bipolar and healthy subjects in brain metrics, differences in amygdala nodal centrality were not present at baseline, but were evident after 8 weeks of treatment. The decrease of topological centrality of amygdala in manic patients is of interest given the recognized importance of this region in bipolar illness [46, 47]. The amygdala changes were later emerging (only at week 8) than most other treatment-related changes, and to not differ between drug treatments. These findings may be of clinical interest, but in the timing and nature of this effect, as it suggests a reduced integration of the amygdala with broader brain networks after treatment. The psychological consequence of such a change might be to tune down the bottom-up affective salience of life events on neocortical network function.

Consistent with prior studies [48, 49], we found that treatment with medications commonly used in psychiatric patient care can have a significant acute impact on structural brain network properties in patients with BD. Medications used to treat patients with BD have diverse effects on receptor and neuronal processes, but mechanisms of their effects on widely-distributed brain networks remain less well understood. Treatment mechanisms of lithium include inhibition of GSK3, increased expression of neurotrophins, and decreased expression of AMPA receptors [50]. Effects of quetiapine include antagonism on D2 and 5-HT2 receptors and others [51]. Inducing changes in receptor-mediated effects alters the functional activity of neurons, with downstream effects on other neurons with which they interact in brain networks. These changes in neuronal activity can induce changes in proliferation, differentiation, and myelination to alter neuronal microstructure with effects that in aggregate can impact regional cortical thickness [52]. The lack of significant differences in treatment effects between our two study drugs that have quite different pharmacological effects suggests that our findings may represent aspects of the final common pathway of effective

pharmacological treatments for bipolar disorder rather than features specific to either study drug.

The potential clinical utility of identifying neuroimaging biomarkers of treatment response in bipolar disorder has been increasingly recognized [53–55]. There are several independent aspects of biomarker development, with most early machine learning studies focusing on case-control differentiation. However, there may be greater clinical utility to the prediction of treatment outcome. In this study, we found that connectome matrices provided a more accurate prediction of treatment response than regional data directly derived from preprocessed smoothed gray matter images. The prediction model using preprocessed smoothed gray matter images showed 75% sensitivity and 42% specificity, while using connectome-wide matrices we observed lower sensitivity (57%) but high specificity (91%). Thus, the method using preprocessed smoothed gray matter images performed better in detecting true positives (i.e., the true responders) while the method using connectome-wide matrices performed better in detecting true negatives (i.e., the true non-responders). While noteworthy and statistically significant, utility of connectome measures for predicting treatment outcome remains less than required for clinical application at this point. And, our findings failed to identify connectome features that differentially predicted response to the two study medications.

While this is one of the first studies to examine the clinical relevance of structural connectome alterations in bipolar disorder, there are several important limitations. As noted, the significance of nodal centrality differences did not survive application of an FDR threshold of $q = 0.05$, though the aggregate findings and treatment-related changes in anterior and posterior cingulate gyri are of interest. Second, brain parcellation template selection may affect network analysis results, as different templates may lead to different estimates of graph theory parameters [56]. Third, the machine learning method is exploratory; optimal resolution/reduction of features for machine learning studies remains to be established, and including higher or lower numbers of input features may lead to somewhat different solutions—evaluating the possible impact of alternative feature selection strategies on results awaits future studies. Finally, two major questions remain to be addressed: what are the specific neural changes that occurred that led to the connectome-level changes, and what are the cognitive and behavioral changes related to the connectome changes, and do they persist over the course of long-term treatment. Examining the relation of structural and functional connectome changes may be particularly informative, structural connectomics have modest correspondence to brain functional networks in patients with bipolar [57].

In conclusion, the present study provides evidence of global network alterations in bipolar disorder during acute mania. Our observation of baseline connectome abnormalities provides neuroanatomic evidence for distributed dysconnectivity during acute episodes of mania, and novel evidence that these alterations can be normalized with widely used therapeutics for mania and are associated with symptomatic improvement. The potential clinical relevance of these findings is emphasized by the particularly strong specificity in predicting treatment response, as well as by the similarities in findings between subjects receiving quetiapine and lithium. An increasing number of studies have shown that morphological covariance networks can exhibit adaptive reorganization in various brain disorders, and our findings indicate that such clinically-relevant changes in anatomic measures can occur over the course of acute treatment [58–60]. Taken together, these studies suggest that morphological covariance networks are a clinically meaningful way to identify illness-related brain features of bipolar illness. Such structural connectome measures may significantly contribute to the development of improved imaging models to better track and predict treatment outcome in bipolar disorder.

REFERENCES

- DelBello MP, Strakowski SM. Neurochemical predictors of response to pharmacologic treatments for bipolar disorder. *Curr Psychiatry Rep.* 2004;6:466–72.
- Zhang W, Nery FG, Tallman MJ, Patino LR, Adler CM, Strawn JR, et al. Individual prediction of symptomatic converters in youth offspring of bipolar parents using proton magnetic resonance spectroscopy. *Eur Child Adolesc Psychiatry.* 2021;30:55–64.
- Collin G, van den Heuvel MP, Abramovic L, Vreeker A, de Reus MA, van Haren NE, et al. Brain network analysis reveals affected connectome structure in bipolar I disorder. *Hum Brain Mapp.* 2016;37:122–34.
- Skåtun KC, Kaufmann T, Brandt CL, Doan NT, Alnæs D, Tønnesen S, et al. Thalamo-cortical functional connectivity in schizophrenia and bipolar disorder. *Brain Imaging Behav.* 2018;12:640–52.
- Wei Y, Chang M, Womer FY, Zhou Q, Yin Z, Wei S, et al. Local functional connectivity alterations in schizophrenia, bipolar disorder, and major depressive disorder. *J Affect Disord.* 2018;236:266–73.
- Borgelt L, Strakowski SM, DelBello MP, Weber W, Eliassen JC, Komoroski RA, et al. Neurophysiological effects of multiple mood episodes in bipolar disorder. *Bipolar Disord.* 2019;21:503–13.
- Fleck DE, Welge JA, Eliassen JC, Adler CM, DelBello MP, Strakowski SM. Factor analysis of regional brain activation in bipolar and healthy individuals reveals a consistent modular structure. *J Affect Disord.* 2018;234:14–19.
- Passarotti AM, Sweeney JA, Pavuluri MN. Fronto-limbic dysfunction in mania pre-treatment and persistent amygdala over-activity post-treatment in pediatric bipolar disorder. *Psychopharmacol (Berl).* 2011;216:485–99.
- Strakowski SM, Fleck DE, Welge J, Eliassen JC, Norris M, Durling M, et al. fMRI brain activation changes following treatment of a first bipolar manic episode. *Bipolar Disord.* 2016;18:490–501.
- Lippard ETC, Weber W, Welge J, Adler CM, Fleck DE, Almeida J, et al. Variation in rostral anterior cingulate functional connectivity with amygdala and caudate during first manic episode distinguish bipolar young adults who do not remit following treatment. *Bipolar Disord.* 2021;23:500–8.
- Bullmore E, Sporns O. Complex brain networks: graph theoretical analysis of structural and functional systems. *Nat Rev Neurosci.* 2009;10:186–98.
- Biswal BB, Mennes M, Zuo XN, Gohel S, Kelly C, Smith SM, et al. Toward discovery science of human brain function. *Proc Natl Acad Sci USA.* 2010;107:4734–39.
- Leow A, Ajilore O, Zhan L, Arienzo D, GadElkarim J, Zhang A, et al. Impaired inter-hemispheric integration in bipolar disorder revealed with brain network analyses. *Biol Psychiatry.* 2013;73:183–93.
- Forde NJ, O'Donoghue S, Scanlon C, Emsell L, Chaddock C, Leemans A, et al. Structural brain network analysis in families multiply affected with bipolar I disorder. *Psychiatry Res.* 2015;234:44–51.
- Alexander-Bloch A, Giedd JN, Bullmore E. Imaging structural co-variance between human brain regions. *Nat Rev Neurosci.* 2013;14:322–36.
- Chen T, Kendrick KM, Wang J, Wu M, Li K, Huang X, et al. Anomalous single-subject based morphological cortical networks in drug-naïve, first-episode major depressive disorder. *Hum Brain Mapp.* 2017;38:2482–94.
- Niu R, Lei D, Chen F, Chen Y, Suo X, Li L, et al. Disrupted grey matter network morphology in pediatric posttraumatic stress disorder. *Neuroimage Clin.* 2018;18:943–51.
- Zhang W, Lei D, Keedy SK, Ivleva EI, Eum S, Yao L, et al. Brain gray matter network organization in psychotic disorders. *Neuropsychopharmacology.* 2020;45:666–74.
- Sporns O, Tononi G, Kötter R. The human connectome: A structural description of the human brain. *PLoS Comput Biol.* 2005;1:e42.
- Qi S, Meesters S, Nicolay K, Ter Haar Romeny BM, Ossenblok P. Structural brain network: what is the effect of life optimization of whole brain tractography? *Front Comput Neurosci.* 2016;10:12.
- Suo XS, Lei DL, Li LL, Li WL, Dai JD, Wang SW, et al. Psychoradiological patterns of small-world properties and a systematic review of connectome studies of patients with 6 major psychiatric disorders. *J Psychiatry Neurosci.* 2018;43:427.
- Cao M, Wang Z, He Y. Connectomics in psychiatric research: advances and applications. *Neuropsychiatr Dis Treat.* 2015;11:2801–10.
- Collin G, de Nijs J, Hulshoff Pol HE, Cahn W, van den Heuvel MP. Connectome organization is related to longitudinal changes in general functioning, symptoms and IQ in chronic schizophrenia. *Schizophr Res.* 2016;173:166–73.
- Kong XZ, Wang X, Huang L, Pu Y, Yang Z, Dang X, et al. Measuring individual morphological relationship of cortical regions. *J Neurosci Methods.* 2014;237:103–7.
- Wang H, Jin X, Zhang Y, Wang J. Single-subject morphological brain networks: connectivity mapping, topological characterization and test-retest reliability. *Brain Behav.* 2016;6:e00448.
- Xia M, Womer FY, Chang M, Zhu Y, Zhou Q, Edmiston EK, et al. Shared and distinct functional architectures of brain networks across psychiatric disorders. *Schizophr Bull.* 2019;45:450–63.

27. Kaufman J, Birmaher B, Brent D, Rao U, Flynn C, Moreci P, et al. Schedule for affective disorders and schizophrenia for school-age children-present and lifetime version (K-SADS-PL): initial reliability and validity data. *J Am Acad Child Adolesc Psychiatry*. 1997;36:980–88.
28. Young RC, Biggs JT, Ziegler VE, Meyer DA. A rating scale for mania: reliability, validity and sensitivity. *Br J Psychiatry*. 1978;133:429–35.
29. Strakowski SM, Eliassen JC, Lamy M, Cerullo MA, Allendorfer JB, Madore M, et al. Functional magnetic resonance imaging brain activation in bipolar mania: evidence for disruption of the ventrolateral prefrontal-amygdala emotional pathway. *Biol Psychiatry*. 2011;69:381–88.
30. Lee JH, Garwood M, Menon R, Adriany G, Andersen P, Truwit CL, et al. High contrast and fast three-dimensional magnetic resonance imaging at high fields. *Magn Reson Med*. 1995;34:308–12.
31. Davis AK, DelBello MP, Eliassen J, Welge J, Blom TJ, Fleck DE, et al. Neurofunctional effects of quetiapine in patients with bipolar mania. *Bipolar Disord*. 2015;17:444–49.
32. Ashburner J, Friston KJ. Unified segmentation. *Neuroimage*. 2005;26:839–51.
33. Tzourio-Mazoyer N, Landeau B, Papathanassiou D, Crivello F, Etard O, Delcroix N, et al. Automated anatomical labeling of activations in SPM using a macroscopic anatomical parcellation of the MNI MRI single-subject brain. *Neuroimage*. 2002;15:273–89.
34. Rubinov M, Sporns O. Complex network measures of brain connectivity: uses and interpretations. *Neuroimage*. 2010;52:1059–69.
35. Watts DJ, Strogatz SH. Collective dynamics of 'small-world' networks. *Nature*. 1998;393:440–2.
36. He Y, Dagher A, Chen Z, Charil A, Zijdenbos A, Worsley K, et al. Impaired small-world efficiency in structural cortical networks in multiple sclerosis associated with white matter lesion load. *Brain: a J Neurol*. 2009;132:3366–79.
37. Zhang J, Wang J, Wu Q, Kuang W, Huang X, He Y, et al. Disrupted brain connectivity networks in drug-naive, first-episode major depressive disorder. *Biol Psychiatry*. 2011;70:334–42.
38. Achard S, Bullmore E. Efficiency and cost of economical brain functional networks. *PLoS Comput Biol*. 2007;3:e17.
39. Jung WH, Yücel M, Yun JY, Yoon YB, Cho KI, Parkes L, et al. Altered functional network architecture in orbitofronto-striato-thalamic circuit of unmedicated patients with obsessive-compulsive disorder. *Hum Brain Mapp*. 2017;38:109–19.
40. Freeman LC. A set of measures of centrality based on betweenness. *Sociometry*. 1977;40:35–41.
41. Long Z, Duan X, Xie B, Du H, Li R, Xu Q, et al. Altered brain structural connectivity in post-traumatic stress disorder: a diffusion tensor imaging tractography study. *J Affect Disord*. 2013;150:798–806.
42. Ma S, Calhoun VD, Eichele T, Du W, Adali T. Modulations of functional connectivity in the healthy and schizophrenia groups during task and rest. *Neuroimage*. 2012;62:1694–704.
43. Borchardt V, Lord AR, Li M, van der Meer J, Heinze HJ, Bogerts B, et al. Preprocessing strategy influences graph-based exploration of altered functional networks in major depression. *Hum Brain Mapp*. 2016;37:1422–42.
44. Foland-Ross LC, Thompson PM, Sugar CA, Madsen SK, Shen JK, Penfold C, et al. Investigation of cortical thickness abnormalities in lithium-free adults with bipolar I disorder using cortical pattern matching. *Am J Psychiatry*. 2011;168:530–9.
45. Rimol LM, Hartberg CB, Nesvåg R, Fennema-Notestine C, Hagler DJ Jr., Pung CJ, et al. Cortical thickness and subcortical volumes in schizophrenia and bipolar disorder. *Biol Psychiatry*. 2010;68:41–50.
46. Townsend J, Altschuler LL. Emotion processing and regulation in bipolar disorder: a review. *Bipolar Disord*. 2012;14:326–39.
47. Delvecchio G, Fossati P, Boyer P, Brambilla P, Falkai P, Gruber O, et al. Common and distinct neural correlates of emotional processing in Bipolar Disorder and Major Depressive Disorder: a voxel-based meta-analysis of functional magnetic resonance imaging studies. *Eur Neuropsychopharmacol*. 2012;22:100–13.
48. Lei D, Li W, Tallman MJ, Patino LR, McNamara RK, Strawn JR, et al. Changes in the brain structural connectome after a prospective randomized clinical trial of lithium and quetiapine treatment in youth with bipolar disorder. *Neuropsychopharmacology*. 2021;46:1315–23.
49. Li W, Lei D, Tallman MJ, Patino LR, Gong Q, Strawn JR, et al. Emotion-related network reorganization following fish oil supplementation in depressed bipolar offspring: an fMRI graph-based connectome analysis. *J Affect Disord*. 2021;292:319–27.
50. Hashimoto R, Takei N, Shimazu K, Christ L, Lu B, Chuang DM. Lithium induces brain-derived neurotrophic factor and activates TrkB in rodent cortical neurons: an essential step for neuroprotection against glutamate excitotoxicity. *Neuropharmacology*. 2002;43:1173–9.
51. Maan JS, Ershadi M, Khan I, Saadabadi A. Quetiapine. *StatPearls* [Internet]. StatPearls Publishing; 2021.
52. Thornton MA, Hughes EG. Neuron-oligodendroglia interactions: Activity-dependent regulation of cellular signaling. *Neurosci Lett*. 2020;727:134916.
53. Lim CS, Baldessarini RJ, Vieta E, Yucel M, Bora E, Sim K. Longitudinal neuroimaging and neuropsychological changes in bipolar disorder patients: review of the evidence. *Neurosci Biobehav Rev*. 2013;37:418–35.
54. Ketter TA, Wang PW. Predictors of treatment response in bipolar disorders: evidence from clinical and brain imaging studies. *J Clin Psychiatry*. 2002;63:21–5.
55. Lei D, Qin K, Li W, Pinaya WHL, Tallman MJ, Patino LR, et al. Brain morphometric features predict medication response in youth with bipolar disorder: a prospective randomized clinical trial. *Psychol Med*. 2022:1–11.
56. Wang J, Wang L, Zang Y, Yang H, Tang H, Gong Q, et al. Parcellation-dependent small-world brain functional networks: a resting-state fMRI study. *Hum Brain Mapp*. 2009;30:1511–23.
57. Luciw NJ, Toma S, Goldstein BI, MacIntosh BJ. Correspondence between patterns of cerebral blood flow and structure in adolescents with and without bipolar disorder. *J Cereb Blood Flow Metab*. 2021;41:1988–99.
58. He Y, Chen Z, Evans A. Structural insights into aberrant topological patterns of large-scale cortical networks in Alzheimer's disease. *J Neurosci*. 2008;28:4756–66.
59. Zhang Y, Lin L, Lin CP, Zhou Y, Chou KH, Lo CY, et al. Abnormal topological organization of structural brain networks in schizophrenia. *Schizophr Res*. 2012;141:109–18.
60. Seeley WW, Crawford RK, Zhou J, Miller BL, Greicius MD. Neurodegenerative diseases target large-scale human brain networks. *Neuron*. 2009;62:42–52.

AUTHOR CONTRIBUTIONS

DL and WBL analyzed the image data and drafted the manuscript. MJT, LRP, JAW, JRS, ER, FGN, DEF, SMS, MPD, and CMA designed the study and collected clinical and image data. SL, QYG, and JAS contributed to data analysis and manuscript writing. All authors reviewed and approved the manuscript for submission.

FUNDING

This research was supported by NIMH grants P50MH077138, R01MH080973, and R01MH078043; and a grant from AstraZeneca Pharmaceuticals. Funding sources had no role in the design and conduct of this study; collection, management, analysis, and interpretation of the data; preparation, review, approval of the manuscript; or decision to submit the manuscript for publication.

COMPETING INTERESTS

FGN spouse is an employee at Eli Lilly and Co. FGN himself reported no conflicts of interests. JRS has received research support from the National Institutes of Health (NIMH/NIEHS/NICHD) as well as AbbVie, Neuronetics, and Otsuka. He has received material support from and provided consultation to Myriad Genetics and receives royalties from the publication of two texts (Springer) and serves as an author for UpToDate and an Associate Editor for Current Psychiatry. He has spoken in CME presentations for Neuroscience Education Institute, MedScape, American Academy of Child & Adolescent Psychiatry, American Academy of Pediatrics, and CMEology. Finally, JRS also has provided consultation to the FDA and Intracellular Therapeutics. JAS consults to VeriSci. LRP has received research support from Acadia, Allergan, Janssen, Johnson and Johnson, Lundbeck, Otsuka, Pfizer, Sunovion and Supernus. MPD is on the lecture bureau for Sunovion; has received research support from Alkermes, Acadia, Allergan, Janssen, Johnson and Johnson, Lundbeck, Otsuka, Pfizer, Sunovion and Supernus; and has provided consultation or advisory board services for Alkermes, Allergan, Assurex, CMEology, Janssen, Johnson and Johnson, Lundbeck, Myriad, Neuronetics, Otsuka, Pfizer, Sunovion and Supernus. CMA has spoken for Otsuka and Janssen. He has received research support from Merck, Forest, and Alkermes, and provided consultation for Janssen. SMS chairs Data Safety and Monitoring Boards for Sunovion and has grant funding (through the University of Texas) from Janssen. All other authors declare that they have no potential conflicts of interest.

ADDITIONAL INFORMATION

Supplementary information The online version contains supplementary material available at <https://doi.org/10.1038/s41386-022-01328-y>.

Correspondence and requests for materials should be addressed to Du Lei.

Reprints and permission information is available at <http://www.nature.com/reprints>

Publisher's note Springer Nature remains neutral with regard to jurisdictional claims in published maps and institutional affiliations.